Texas Erosion Analysis Model: Theory and Validation

Udai B. Singh, James M. Gregory and Gregory R. Wilson

Introduction

Detachment and transport of soil due to the natural force of wind is a major agricultural and environmental problem in many parts of the world. Atmospheric Loading of dust caused by wind erosion also affects human health and environmental air quality. There is a high on-site as well as off-site cost due to wind erosion. Wind erosion reduces soil productivity, decreases agricultural production, and deteriorates soil quality. Sediments from wind erosion fill up irrigation canals and road ditches, cover the railroads and roads, cause household dust damages, and affect the water quality of rivers and streams. The dust production reduces visibility on highways, affects human health, and pollute the air.

In order to conserve the soil (the most valuable natural resource) and protect the human health and environment, it is very much necessary to understand and control the wind erosion process. Texas Erosion Analysis Model (TEAM) developed at the Wind Engineering Research Center, Texas Tech University, Lubbock, Texas, is a mathematical model which simulates the detachment and maximum transport rate of soil and associated dust loading to the environment. The model is based on understanding of physical processes related to wind erosion and can be used as a analysis tool to design the methods and management practices to control wind erosion.

Key elements of TEAM are wind profile and friction velocity, soil cover factor, threshold friction velocity, soil detachment function, maximum transport rate equation, eroding field length effects on wind erosion, soil erodibility, mechanics of dust generation, saltation height and reference zone concentration, dust concentration with height, and visibility prediction. An overview of theoretical development and experimental validation of these key elements of physics of wind erosion are described in this paper.

Wind Erosion Process

Wind erosion and associated dust generation are energy driven processes. Wind is the energy source and the energy is transferred to the soil surface through fluid shear and energy of saltating particles. If the soil surface is covered by residues, plant canopies or stable aggregates such as clods and rocks, the energy transfer is reduced. To sustain the wind erosion process, the available energy from wind must exceed the threshold requirements of loose soil particles. Threshold friction velocity is a measure of threshold requirements and it is a function of particle size and liquid bonder content and type. For water, atmospheric relative humidity controls the liquid contents of soil surface.

TEAM is comprised of two functions which describe the mechanism of wind erosion and dust generation. The first function determines the detachment and maximum transport rate and is highly sensitive to wind speed, vegetative cover, surface residue, soil aggregate cover, soil particle size distribution, and soil moisture. The second function describes the change in soil movement associated with the transition of the land surface from one dominated by a solid mass or large aggregates to one dominated by loose sand or sand-like aggregates. Effect of field length and aggregate abrasion due to saltating particles are the processes related to dust generation and environmental air pollution.

Various physical processes act and interact to govern the rate of soil movement by wind. Wind erosion can be viewed as the interaction of three energy components: wind (energy), soil (energy resistance), and plant cover and surface roughness (energy reduction). The magnitude of the wind velocity at a specified height and the shape of the wind profile determines the rate at which energy is transferred to the field surface (Figure 1). Soil particles can only move if wind energy is sufficient to overcome both gravity and inter-particle cohesion. Soil aggregates too large to move behave as a solid mass and act as cover at the interface zone to protect small loose particles from wind energy. Cover from aggregates and plant residue protects soil from wind erosion by reducing the energy intensity at the bottom of the wind profile (top of the interface zone). Air trapped between clods and other cover elements reduces the energy intensity at the base of the interface zone. Energy reduction is proportional to the fraction of cover and the inverse of the interface zone thickness squared (Gregory, 1984a). The roughness at the field surface causes drag on the wind and controls the shape of the wind profile. Changes at the plant and soil surface affect both the wind profile and the energy transferred to the loose soil at the field surface.

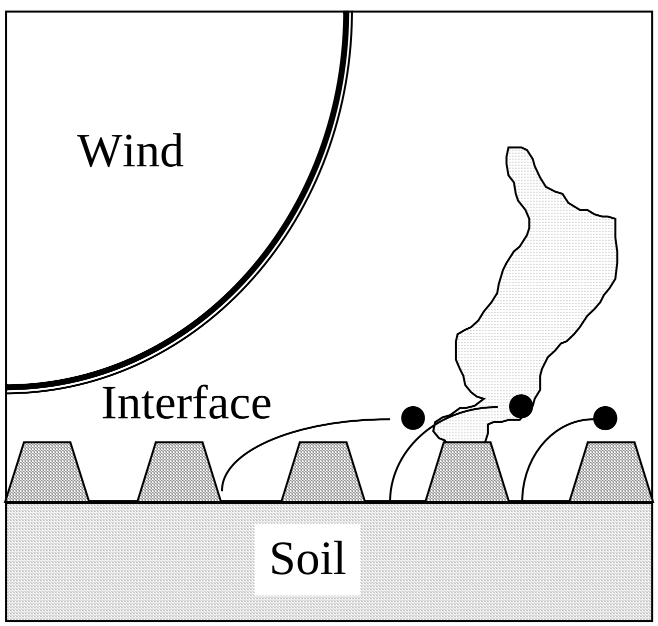

Figure 1. Interaction of wind, cover, and soil (Gregory et al. 1996).

Wind Profile and Friction Velocity

Wind is the kinetic energy source for the detachment and transport processes. The force component of the work to detach soil is obtained from the fluid shear stress associated with the shape of the wind profile; however, the most convenient term to use is the friction velocity, defined as the square root of the ratio of fluid shear stress to fluid density. Heating or cooling at the land surface can cause differences in air density and affect the shape of the profile; however, if winds are strong enough to exceed threshold for the movement of sand and dust, turbulent mixing usually eliminates the density difference resulting in a neutral boundary layer (Greeley and Iversen, 1985). Abtew et al. (1989) described that the friction velocity for neutral profile conditions can be obtained with the following equation:

$$U_* = \frac{0.4U_z}{\ln\left[(Z - D) / Z_o\right]} \qquad (1)$$

where U_* = friction velocity (m/s),
U_Z = wind velocity at height Z (m/s),
Z = height above the soil surface at which wind velocity is measured (m),
D = displacement height (average height of the roughness elements, m), and
Z_o = aerodynamic roughness (m).

The aerodynamic roughness is the elevation difference between the average surface roughness and the height of the extrapolated intercept of the log relationship where wind velocity approaches zero. The displacement height is the elevation difference between the lower surface base, such as the bottom of a ridge, or the soil base from which aggregates protrude. It is the average height of roughness elements. The total distance of Z_o and D, is the amount that the wind profile is displaced above the soil base.

To predict the displacement height, Abtew et al. (1989) derived the following equation :

$$D = F_c\, H_a \qquad (2)$$

where F_c = the fraction of cover by the roughness elements, and
H_a = the average height of the roughness elements (m).

The following two equations can be used to estimate the aerodynamic roughness (Gregory, 1991):

$$Z_{ors} = 0.13\left(H_m - D\right) \qquad (3)$$

where H_m = maximum height of elements providing the major cover and

$$Z_o = Z_{ors} + \left[0.13\left(H_{ms} - D_s\right) - Z_{ors}\right]\left[1 - \exp^{-Xs}\right] \quad (4)$$

where X_s = $(H_{ms}\ W_e)/S_e^2$
Z_{ors} = the aerodynamic roughness for a surface with 0.3 or more fraction of cover by elements (Z_{ors} is predicted with Equation 3 using H_m and D for the elements that provide the major cover) (m),
H_{ms} = the maximum height of sparse cover elements (tallest elements in system)(m),
D_s = the displacement height of all elements including the sparse elements (m),
W_e = the width of sparse elements (m), and
S_e = spacing of sparse elements (centerline to centerline)(m).

On relatively smooth land surfaces, the addition of saltation particles to the air mass just above the surface will cause the wind profile to adjust its shape. The most pronounced effect is the increase in displacement height. Displacement height can generally increase from less than a centimeter to 0.015-0.02 m depending on the wind velocity and the mass of soil moving in saltation (Wilson et al., 1993b). This increase in displacement height will generally increase the magnitude of U_*. While this effect is easily detected in wind tunnel studies, the effect is usually less pronounced for the field conditions because the land surface roughness causes an initial displacement height in the 0.01-0.02 m range. The work of Abtew et al. (1989) seems to match field conditions reasonably well; however, additional detailed investigations on the effect of saltation particles on the shape of the wind profile are probably justified.

Soil Cover Factor

The concept of relative soil loss as a function of canopy and residue cover for water and wind erosion was introduced by Gregory (1984a) and termed as soil cover factor which expresses the fraction of wind energy that reaches to the eroding soil surface. The soil cover factor is analogues to the C factor of Universal Soil Loss Equation for water erosion. Equation 5 was derived and developed by Gregory (1984a) to predict relative energy as a function of fraction and height of cover:

$$S = \frac{1 - F_r}{\left[1 + \left(\frac{h_r}{h_s} - 1\right)F_r\right]^2} \quad (5)$$

where S = cover factor, which expresses the fraction of wind energy that reaches the eroding soil surface,
F_r = fraction of cover,
h_r = height of cover (m), and
h_s = height of soil roughness (m).

The standard deviation of random roughness data in real space can be used to determine the height of soil roughness. It is possible that distortion may occur if data are analyzed in log space. Equation 5 has been validated by field data and predicts the relative soil loss for wind erosion for variation in ridge height and clod cover with an R^2=0.99 (Gregory, 1984a).

The following relationship derived by Gregory (1982) can be used to estimate the fraction of cover from mass/area of residue cover:

$$F_r = 1 - exp^{-A_m M_a} \qquad (6)$$

where A_m = a coefficient that expresses the area covered per unit mass for one piece of residue (ha/kg), and

M_a = the mass per area of residue on the field (kg/ha).

The coefficient, A_m, varies with type of residue material and climate type. The same type of plant will often have smaller values of A_m in dry climates as opposed to more humid ones. The predicted reduction in soil loss from Equations 5 and 6 are shown with measured values in Figure 2. Soil cover factor is one of the most important variables that affect the transfer of wind energy to the soil and ultimately reduces soil movement.

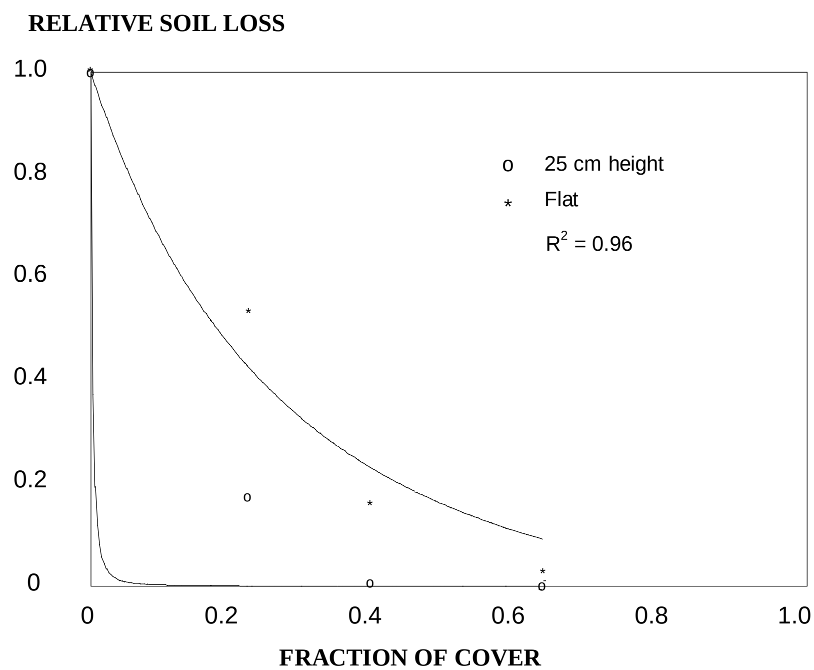

Figure 2. Relative soil loss as a function of fraction of cover predicted from mass/area of residue cover. Data from Chepil and Woodruff (1963).

Threshold Friction Velocity

A classical equation for threshold friction velocity was derived by Bagnold (1941). The relationship is a square-root function of particle diameter (for particle diameter larger than about

0.1 mm). The relationship derived by Bagnold (1941) is adequate for arid regions but the effect of soil moisture is a major factor in semi-arid and sub-humid regions. Bagnold's relationship was expanded by Gregory and Darwish (1990) to include the effect of electrostatic bonding (for small diameter particles) and soil moisture. The equation is as follows:

$$U_{*t} = 0.118\left[21.2D_{50}\left(1+0.01W_a+\frac{0.0045}{{D_{50}}^2}+\frac{1.2}{D_{50}}exp^{-0.1\frac{W_a}{W_w}}\left(W_a-W_c\right)\right)\right]^{0.5} \quad (7)$$

where D_{50} = mean particle diameter of primary soil particle size distribution (mm),
W_a = soil water content expressed as a percentage,
W_w = wilting point of soil expressed as a percentage, and
W_c = water attached to clay, in scratches on the particle surface, or internal to the surface of the particle expressed as a percentage.

The relationship between W_c and the wilting point (W_p) can be determined from the data and statements by Chepil (1956) and Bisel and Hsieh (1966). Chepil states that erodibility by wind is about the same for soil that is oven dried or air-dried in the sun or in shade when moisture did not exceed one-third of 15 atmosphere percentage (W_p). Beyond this range of moisture a distinct decrease in erodibility was manifested. Data presented in Figure 3 supports a W_c of $0.5W_p$. Because these data were probably collected using a method that over estimated the measured surface soil moisture, the slope of the line is suspect. Chepil's experiments with sun dried and oven-dried conditions would have the best control of surface moisture. A W_c equal to $1/3W_p$ based on Chepil's observations is recommended.

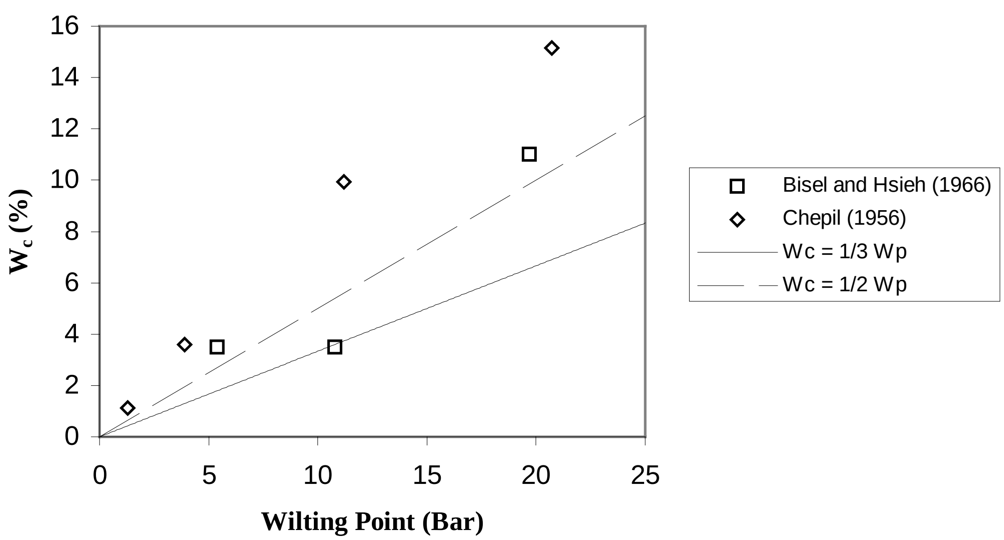

Figure 3. Relationship between wilting point and W_c.

Soil water can be related to relative humidity (Gregory, 1991). The term W_a-W_c is set to zero when W_c exceeds W_a. The effect of particle size and soil moisture on threshold friction velocity is shown in Figure 4.

The details of relationship between soil water content and atmospheric relative humidity can be found in a similar publication by Gregory et al. (1996).

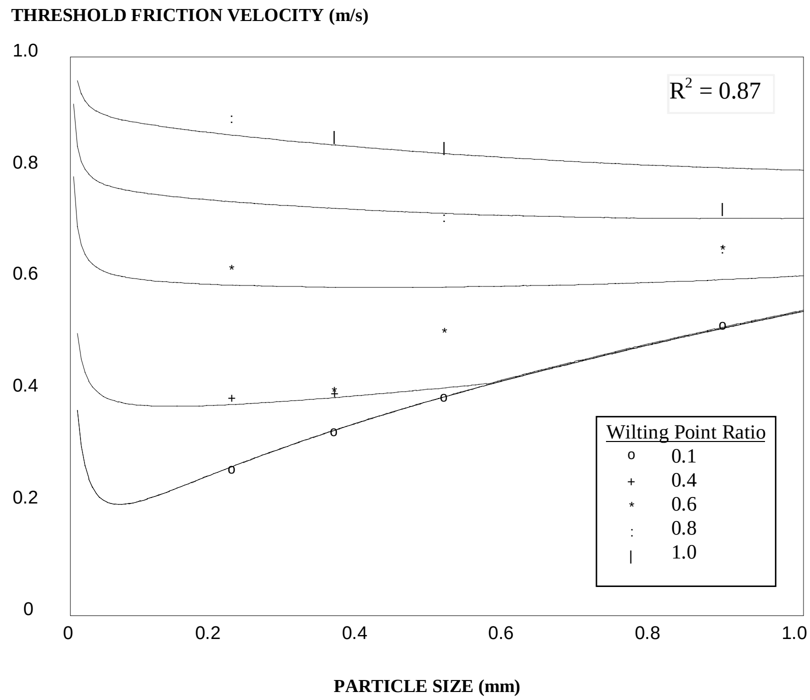

Figure 4. Effect of moisture content on the threshold friction velocity of various sized particles (Source: Darwish, 1991).

Soil Detachment Function

Tillage practices, natural weathering , aggregate abrasion and abrasion due to animal grazing can make soil particles small in size and easy to move. Wind and water erosion both appears to have universal detachment process. Wilson and Gregory (1992) and Gregory (1992) expressed the detachment process by following relationship:

$$m = \left[\left(\frac{\rho_{bs}}{\tau_s} \right) f(\Theta) \right] K_E \qquad (8)$$

where m = mass of soil detached (kg),

ρ_{bs}	=	soil bulk density (kg/m^3),
τ_S	=	soil shear strength (N/m^2),
$f(\Theta)$	=	function of soil shear angle, θ, (dimensionless), and
K_E	=	kinetic energy input (J).

The equation 8 was obtained through dimensional analysis and verified with measured results for wind and water erosion (Wilson and Gregory, 1992).

Maximum Transport Rate Equation

Equation 8 was expanded by Gregory et al. (1993a) to include the evaluation of kinetic energy from the wind profile, cover, and particle size effects. The development is detailed; however, the resulting equation relates detachment to soil strength, particle size, particle size distribution, soil cover, friction velocity, and threshold friction velocity. The resulting detachment equation is as follows:

$$\frac{m}{WLt} = C_1 \rho_f \left(\frac{\rho_{bs}}{\tau_s}\right) \frac{D_{50}}{D_r} \left(1 + C_2 \frac{\sqrt{D_{75}} - \sqrt{0.08}}{\sqrt{D_r}}\right) \left(SU_*^{\,2} - \left(\frac{0.8U_{*t}}{G_f}\right)^2\right) U_* \quad (9)$$

where	W	=	width of eroding surface (m),
	L	=	length of eroding surface (m),
	t	=	time (hr),
	C_1	=	coefficient obtained from calibration (0.004),
	C_2	=	coefficient obtained from calibration (125),
	ρ_f	=	density of fluid (1.23 kg/m^3 for air),
	D_{50}	=	mean particle diameter of primary soil particle size distribution (mm),
	D_r	=	reference particle diameter (1.0 mm),
	D_{75}	=	particle diameter of primary soil particle size distribution at the 75 percentage location (mm),
	U_{*t}	=	threshold friction velocity (m/s), and
	G_f	=	a gust factor (1.5 for field conditions and 1.0 for wind tunnel conditions).

The maximum soil transport rate by wind occurs when the soil surface is completely covered with loose erodible particles. Wilson and Gregory (1992) showed that loose soil shear strength can be equated to the wind shear at threshold conditions. The following equation was developed for loose soil detachment and maximum transport rate with the length of detachment set to unity:

$$\frac{m}{Wt} = 0.004 \rho_{bs} \left(\frac{G_f}{0.8U_{*t}}\right)^2 \frac{D_{50}}{D_r} \left(1 + 125 \frac{\sqrt{D_{75}} - \sqrt{0.08}}{\sqrt{D_r}}\right) \left(SU_*^{\,2} - \left(\frac{0.8U_{*t}}{G_f}\right)^2\right) U_* \; (10)$$

The maximum transport equation was calibrated with published data reported from wind tunnel studies and fit the experimental data with an R^2 of 0.95, which was highly significant (□= 0.001) (Gregory et. al., 1993a). The equation was also tested with field data from Svasek and Terwindt (1974) shown in Figure 5 and data from Nickling (1978) shown in Figure 6. The upper and lower curves were generated with Equation 10 by considering the effect of relative humidity on threshold friction velocity. The two soils also had different particle size distributions. Data from Wilson et al. (1993b) and Wilson (1994) indicate that Equation 10 responds correctly to changes in soil moisture associated with relative humidity, and that the current calibration is reasonable. Data relating soil moisture to relative humidity are available from Puri et al. (1925).

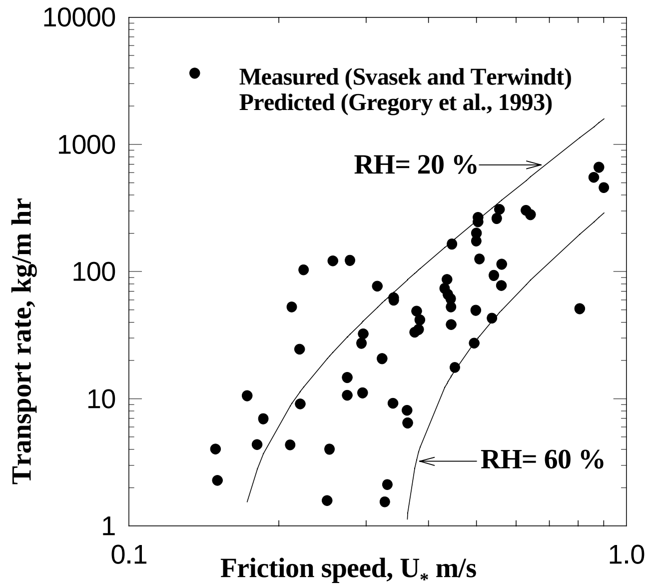

Figure 5. Comparison of measured maximum transport field data and predicted range.

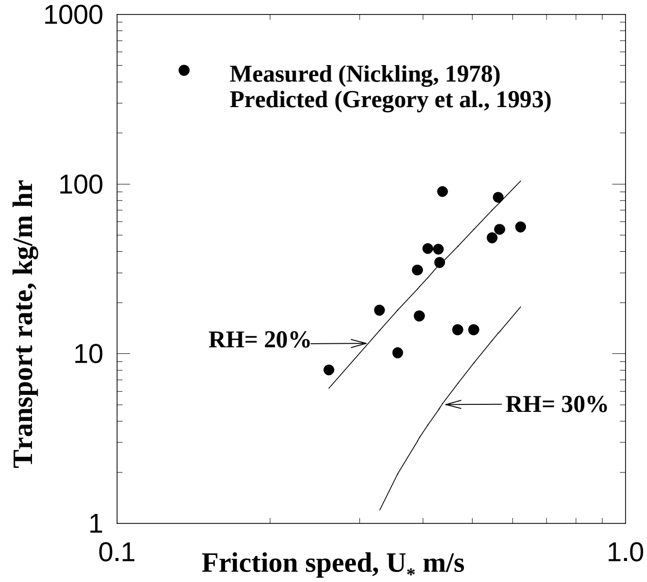

Figure 6. Comparison of measured maximum transport field data and predicted range.

Eroding Field Length Effect on Wind Erosion

Chepil's measurements on the length effect (Chepil, 1957) provided a classic data set that related soil movement to field length and soil type. Bagnold (1936) had investigated the effect of length on sand movement in a wind tunnel; however, the length to maximum movement for sand was only 2 to 4 meters compared to 100's of meters for soil.

A physical explanation for the length effect was first presented by Gregory (1984b). Two principles were identified to explain the process. The first principle is that the change in soil movement across a field is due to the decreased availability of soil for new detachment as the moving loose soil covers the solid soil component. Gregory (1984b) derived the following equation to describe this process for the simplest condition of no incoming sediment at the beginning of the field:

$$L_f = 1 - \exp^{-A_f L \frac{D_t}{D_{tl}}} \tag{11}$$

where L_f = length factor,
D_t = detachment rate of solid soil (kg/m^2-hr),
D_{tl} = detachment rate of loose soil (kg/m^2-hr),
A_f = abrasion factor (dimensionless), and
L = length of field (m).

The dimensionless length factor varies between 0.0 and 1.0. This equation matched measured data reported by Chepil (1957) for a sandy loam soil with an R^2 of 0.93 and was highly significant (□ =0.001). It also matched measurements made in a wind tunnel for pure sand (D_t=D_{tl}) reported by Bagnold (1936) for a friction velocity of 0.92 m/s with an R^2 of 0.95, which was highly significant (□ =0.001). The abrasion factor, A_f, was set to 1.0 for these analysis.

Equation 11 is valid, however, only for sandy soils or pure sand at high winds because it only considers one of the two processes that affect the length relationship. The second principle is related to field length that the total kinetic energy of particles abrading aggregates initially increases exponentially with field length as the number of particles increase. The collision of one loose particle detaches others, and each of them detaches more, etc. At about 35 percent surface cover by loose particles, the solid soil surface becomes sheltered from direct impact from saltating particles. At this point, the exponential growth in the number of particles is curtailed, and the abrasion adjustment factor reaches an upper limit of 1.0. This effect can be considered by multiplying the detachment ratio in Equation 11 by the following abrasion adjustment factor:

$$A_f = 0.1\exp\left(\frac{2.3L}{L+\left(\frac{D_{tl}}{D_t S U_*^{2}}\right)\exp\left[-1.7\left(\frac{D_t S U_*^{2}}{D_{tl}}\right)L\right]}\right) \qquad (12)$$

Equation 12 was developed empirically considering the fact that the number of loose, abrasive particles initially increased exponentially and considering that the equation needed to have an upper limit of 1.0 and be stable for calculations on a computer. The calibration for Equation 12 was obtained with field data from Chepil (1957) and wind tunnel data from Bagnold (1936) for sand movement with a friction velocity of 0.36 m/s. The R^2 obtained form Bagnold's data for this relationship was 0.97 and was highly significant (□=0.001). The relationship also predicts the field results reported by Chepil (1957) as shown in Figure 7. Two problems with Chepil's data are that he did not separate the effects of aggregate size and soil erodibility, and aggregate size and clay content were not reported in enough detail to make a precise calibration or evaluation. Because Equation 12 contains the variable U_*, which varies with wind speed, the length factor should vary during an erosion event, making it difficult to obtain precise data for calibration. Most length relationships presented in the literature do not include the variable of friction velocity; however, controlled measurements by Bagnold (1936) fully verify the necessity of including friction velocity as a variable.

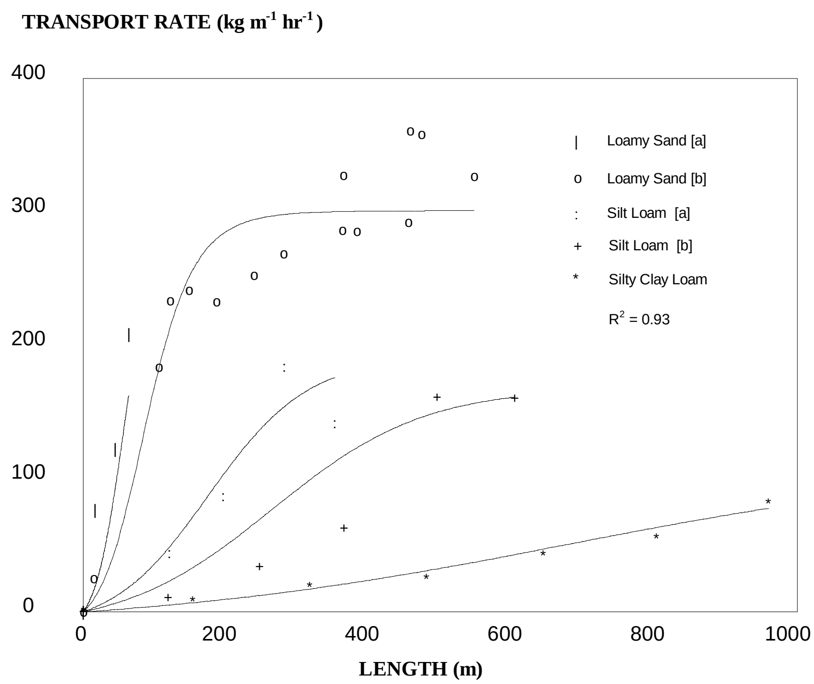

Figure 7. Effect of soil type on the length effect (Data from Chepil, 1957).

Soil Erodibility

In the literature, many different definitions for soil erodibility are found. In this paper soil erodibility will be defined as the mass detached per unit kinetic energy. One key to understanding wind erosion, especially the length effect, is the recognition that at least two soil erodibilities exist: one for cohesive soil and one for loose soil. To detach soil particles from a solid condition, input energy is needed to break the bonding force between particles. To detach loose soil, the input energy only has to overcome the force of gravity and any liquid bonds, such as surface tension.

Wilson and Gregory (1992) defined soil erodibility, E, as

$$E = \frac{\rho_{bs}}{\tau_s} f(\Theta) \qquad (13)$$

where E = erodibility (kg/J).

Loose soil erodibility, E_l, was defined (Wilson and Gregory, 1992) as

$$E_t = N \frac{\rho_{bs}}{\rho_f U_{*t}^{\,2}} \qquad (14)$$

where E_t = loose soil erodibility (kg/J), and
N = a number obtained from calibration.

This understanding of erodibility was used in the development of Equations 9 and 10. Equation 14 also helps in the understanding of the length effect. If the detachment ratio in Equations 12 and 13 is obtained by dividing the right side of Equation 9 by the right side of Equation 10, the following equation is obtained:

$$\frac{D_t}{D_{tl}} = \frac{C_3 \rho_f \rho_{bs} / \tau_s}{0.004 \rho_{bs} \left(\frac{G_f}{0.8 U_{*t}} \right)^2} \tag{15}$$

where C_3 = calibration coefficient.

The detachment ratio is essentially the ratio of erodibilities. Wilson and Gregory (1992) noted that the $\square_s/\square_{bs}$ term had the same dimensions as crushing energy (the energy required to crush a defined mass of cohesive soil) as defined by Skidmore and Powers (1982). A convenient method to estimate soil erodibility for solid soil is crushing energy. Based on limited data, when crushing energy is used, Equation 15 becomes

$$\frac{D_t}{D_{tl}} = \frac{5 \rho_f / E_c}{0.004 \rho_{bs} \left(\frac{G_f}{0.8 U_{*t}} \right)^2} \tag{16}$$

where E_c = crushing energy (J/kg).

Crushing energy, E_c, is approximately a linear function of the percent clay in the soil. Wilson and Gregory (1992), using data from Skidmore and Layton (1992), developed the following equation to estimate E_c as a function of clay percentage:

$$\frac{1}{E_c} = \frac{a1}{Clay_{\%}} \tag{17}$$

where a1 = regression coefficient (1.1).

The length factor prediction shown in Figure 7 used clay content to adjust for soil texture differences. There is some evidence showing that crushing energy is a temporal property of soil and is effected by climate history (Singh et al, 1992; Layton et al., 1993). More research is needed to determine the precise temporal effects. This information could have a major impact on the understanding and prediction of wind erosion, and the implications of climate change on air quality.

Mechanics of Dust Generation

The amount of dust produced, excluding the initial dust already present in the soil system is a byproduct of saltation process during wind erosion. When saltating soil particles returns to the ground, they often hit soil aggregates and other soil particles causing abrasion and emission of fine particles. The process continues to expand as soil particles strike the soil surface and trigger other soil particles into saltation and suspension. The number of soil particles moving in saltation increases with length downwind on eroding field. Therefore, the amount of kinetic energy and the release of dust per unit area also increases with field length. This also confirms the evidence that eroding field length has a secondary effect on the release of dust from saltating particles. Gregory et al. (1993b) developed a general function relating the change in detachment of dust particles to the number of impacts from particle abrasion. The equation is of the following form:

$$\frac{dD}{dN} = -W_f \left(D_p - D\right) \tag{18}$$

where D = dust fraction,
N = number of impacts,
W_f = weathering factor, and
D_p = dust fraction potential.

Equation 18 can be rearranged and integrated from zero to the final dust fraction and from zero impacts to the final number of impacts to obtain

$$\ln\left(\frac{D_p - D}{D_p}\right) = -W_f N \tag{19}$$

Taking the exponential of both sides results in the following form:

$$D = D_p\left(1 - \exp^{-W_f N}\right) \tag{20}$$

Equation 20 predicts that dust generation depends on the potential for dust in the soil fraction and varies with the number of impacts from particle abrasion. If there is initial dust in the soil system from tillage, other mechanical action, or natural weathering, it can be considered with the following equation:

$$D = D_p\left(1 - \exp^{-W_f N}\right) + D_i \tag{21}$$

where D_i = initial dust amount.

Equation 21 was validated and tested with measurements made in the laboratory with a CEDG (Gregory et al., 1993b). Initial results for extremely dry soil conditions are shown in Figure 8. The relationship matched the derived equation with an R^2 of 0.997 and was statistically significant (□ = 0.001). One-thousand rotations are associated with 1600 impacts, which should be equivalent to the number of impacts for particles in saltation to travel 166 m (0.1 miles). A similar results are shown for moist soil. Note that soil moisture inhibits dust generation, as well as, the erosion process.

It is concluded from these results that the number of impacts has a major effect on the release of dust. For field conditions, the number of impacts will depend on field length and the height of saltation, which depends on the wind speed. Obviously, more research is needed to relate the weathering factor to soil type, soil moisture, and other variables that control bonding strength between soil particles. Nevertheless, there is considerable evidence that the loading of dust into the atmosphere can worsen during prolonged droughts (Singh et al., 1992).

The CEDG was also used to study the effects of soil type on dust generation (Singh, 1994). There is significant difference in dust generation between soils dominated by sand, silt, or clay, The type of soil and its sand and clay fractions also affect the weathering factor as well as the potential dust coefficient. As the amount of sand in soil increases, the potential for dust decreases because the amount of fine particles are limited in the soil. At the same time, if there is an ample amount of fine silt and clay in the soil, the dust potential increases as sand content increases because sand particles act as an abrader in energy/abrasion process. The amount of clay content increases the dust potential but the rate of dust generation decreases because of the fact that clay particles stay in aggregates form.

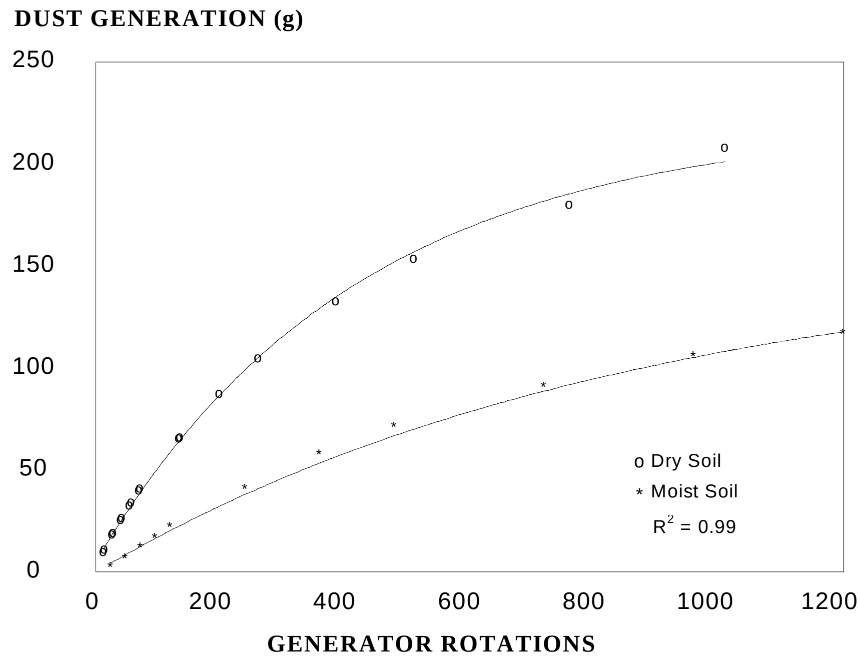

Figure 8. Effect of the number of impacts on the generation of dust from soil.

Saltation Height and Reference Zone Concentration

For a given soil condition and field length, the rate of soil movement, X_s, can be obtained by the product of Equations 10 and 11. The height of saltation for uniform size soil particles can be calculated by setting the potential energy of the particles at the top of trajectory equal to the kinetic energy of particles at shear velocity or friction velocity (U_*), and neglecting the friction in the system. The height of saltation can be determined by following equations:

$$mgH_s = \frac{1}{2} mU_*^{\,2} \qquad (22)$$

to obtain

$$H_s = \frac{U_*^{\,2}}{2g} \qquad (23)$$

where H_s = height of saltation (m), and
g = gravity (m/s^2).

Equation 23 is similar to the results of Owen (1964); however, experimental measurements using highly efficient isokinetic samplers in the wind tunnel at Texas Tech University do not verify this relationship (Wilson et al., 1993b). The measured average heights of saltation are within 1 cm of the predicted values of Equation 23, but tends to follow a linear function of U_*, rather than a square relationship. A more detailed and general function to determine the saltation height as a function of particle size and material property can be found in Singh (1994).

The flow rate of air in the saltation layer (dust generation layer) is calculated with the following equation:

$$Q_a = 5.1(H_s)(U_*^{\,2})(W)3600 \qquad (24)$$

where Q_a = air flow rate (m^3/hr).

The value of 5.1 U_* defines the wind velocity at the top of the roughness elements (Gregory et al., 1993a).

Concentration of sediments in the saltation layer is obtained by dividing the mass per time times width by the air flow rate from Equation 24:

$$C_s = \frac{X_s W}{Q_a} \qquad (25)$$

where C_s = concentration in the saltation zone (kg/m^3).

Dust Concentration with Height

The average height of reference zone can be calculated by the saltation height divided by 2.0. The dust concentration with height can be predicted with following equation modified from Anderson and Hallet (1986) (Gregory et al., 1991):

$$C_H = C_s \left(\frac{2H}{H_s} \right)^{-\frac{U_s}{0.4U_*}} \tag{26}$$

where C_H = concentration at desired height H (kg/m^3),
H = height at which concentration is predicted (m), and
U_s = particle settling velocity (m/s).

Length of Visibility Prediction

The length of visibility depends on light penetration. Gregory (1987) derived an equation to predict visibility as a function of dust concentration and particle size. The total light penetration through a system of various particle sizes can be predicted by evaluating the probability of penetration through all concentrations of various particle sizes in the system.

$$P_T = \exp^{-1500 \frac{1}{\rho} \sum_{i=1}^{i=n} \frac{C_i}{D_i}} \tag{27}$$

where P_T = fraction of light that directly penetrates a distance of 1.0 m,
C_i = concentration of particles for size class i (kg/m^3),
D_i = average diameter of size class i (mm),
ρ = particle density (2650 kg/m^3),
i = size class, and
n = number of classes.

The effective average particle diameter at a given height can be determined by rearranging Equation 27,

$$D_{eff} = -1500 \frac{1}{\rho} \frac{C_T}{\ln P_T} \tag{28}$$

where D_{eff} = the effective average particle diameter (mm), and
C_T = the total concentration of all particle size classes at the specified height H.

Length of visibility at a given height can then be predicted using the following equation (Gregory, 1987):

$$L_v = \left[\frac{-\ln P \rho}{1500} \right] \frac{D_{eff}}{C_T} \tag{29}$$

where L_v = length of visibility (m).

The factor P is often set to 0.02 (2.0 percent of the light coming from the target), the lower limit of detection with the human eye (Robinson, 1968).

Applications of TEAM

All of the key elements discussed in this paper are included in a computer program written in BASIC that simulates soil erosion, dust generation, and visibility prediction. Input parameters, include average hourly wind from which friction velocity is determined, relative humidity and clay content to determine threshold friction velocity, D_{50} and D_{75} particle size, particle size distribution, surface cover factor, soil erodibility, soil bulk density, and length of the erosion segments from which the soil detachment and transport rate and dust generation are determined. The output includes total soil movement rate, concentration in saltation layer, dust concentration with height, particle size distribution with height, and length of visibility with height. The program can be used to evaluate various field and climatic conditions to predict erosion, dust generation, and visibility.

TEAM was used to analyze the dust storm that caused a major traffic accident in California in 1991. The visibility predictions are shown in Figure 9. This storm was caused by a cold front that moved over the area on the day of the accident. The bottom portion of the graph shows the changes in wind speed and relative humidity as the storm progressed. As the winds increased, the relative humidity dropped. Both changes increased the potential for wind erosion and blowing dust. The major change in both wind speed and relative humidity occurred over a period of about 4 hours; however, the major change in predicted visibility occurred over a period of about 2 hours.

Predictions of visibility were made for bare soil conditions for the particle size distribution associated with the sandy loam soil type at the site of the accident. Predicted visibility for various heights are shown in Figure 9. The highway patrol reported visibility as low as 50 ft (16 m) during the worst part of the storm (Wilson et al., 1993a). Because a driver must respond under dynamic conditions, these predictions were made for a 10 percent observation of the target instead of the 2 percent discussed earlier. These predicted results seem very reasonable for this storm. The simulated values with height illustrate the dynamic nature of dust suspension. Note that the visibility increases with height, or as dust concentrations decreases.

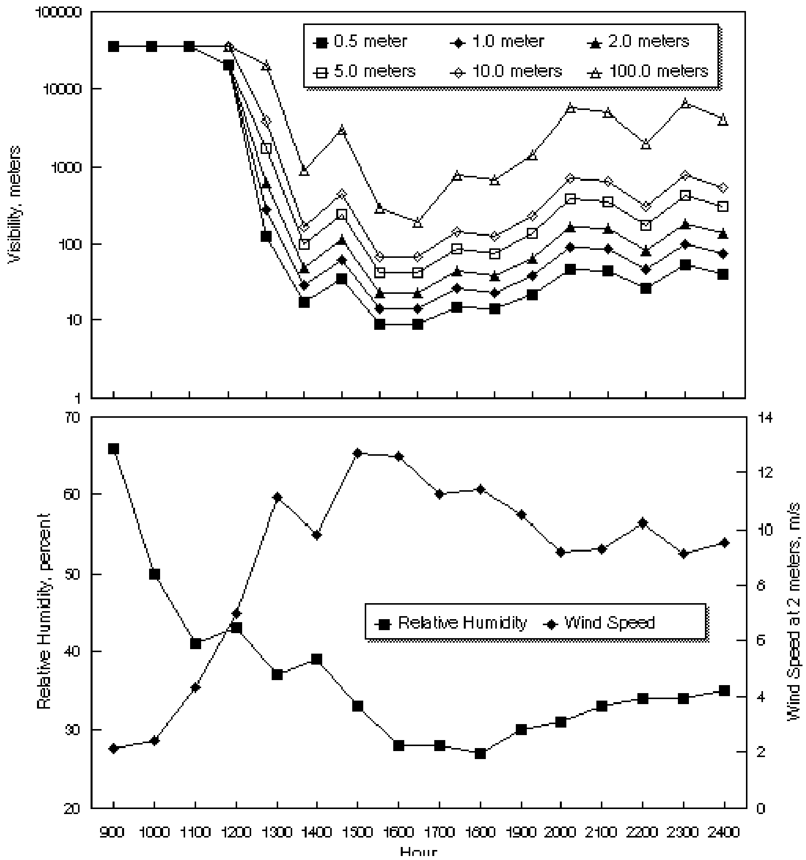

Figure 9. Input weather variables and predicted visibility for a dust storm in California, November, 1991.

The results for a long-term analysis for Lubbock, Texas are shown in Figure 10 (Lee et al., 1993). The measured dust hours represent monthly values averaged over the period from 1947 to 1989 for sightings made at the Lubbock airport. The observer height is about 1.7 m, but the target height is usually higher and often in the range of 10 m. These measurements and simulations illustrate the seasonal variability of blowing dust due to wind, relative humidity, and crop cover variations.

In 1995-1996, TEAM was adopted and is currently in use by a major environmental consulting firm to perform an air quality safety analysis for cleaning up a major environmental contamination site (Pehrson and Chio, 1996).

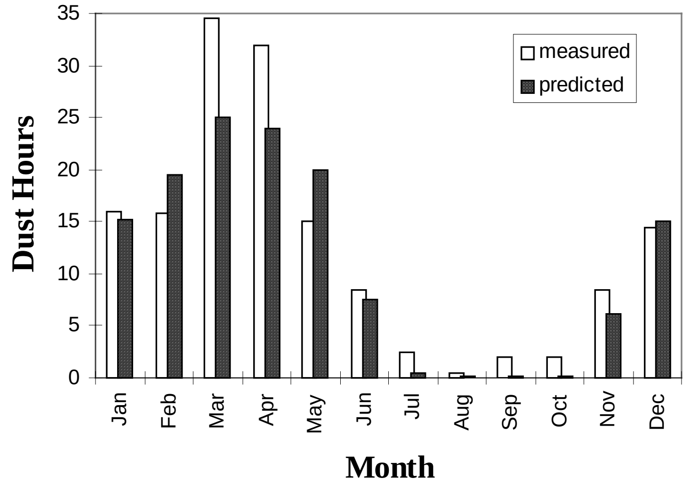

Figure 10. Comparison of measured and predicted long-term dust hours for Lubbock, Texas.

Summary

The process of detachment and transportation of soil by wind and suspension of dust particles affects land and air quality and is an important component in evaluating and establishing environmental management programs. The process begins with the transfer of wind energy through surface cover to the soil. The soil resists the detachment energy until friction velocity exceeds the threshold friction velocity. At this point, loose particles begin to move in saltation. The movement of these particles increases the energy transfer from the wind and triggers and avalanche of particles as they move downwind with field length. Eventually, the soil surface downwind becomes covered with loose sand and or sand-like particles and the movement levels to a maximum transport rate controlled by wind speed, surface cover, soil moisture (relative humidity), particle size, and particle size distribution.

Two soil erodibility values affect the wind erosion process. Soil erodibility for loose soil affects the maximum transport rate. The ratio of soil erodibility of aggregate soil to loose soil erodibility affect the rate of increase in soil movement with field length.

The dust concentration in the saltation zone (zone with initial movement and height of the particles are controlled by the detachment processes) provides the reference concentration to determine the suspension of dust. Particles with low settling velocity tend to go into suspension and are transported upward. The concentration decreases inversely with height. Particles with high settling velocity do not become suspended; they continue to move in the saltation mode. Visibility is dependent on both the concentration and the size of the suspended particles. Visibility is low for high concentrations of small diameter particles.

Because wind erosion and dust generation processes are complex, numerous functions are required to describe all interactions. Many of these functions are presented in this paper. The model which includes all these functions, was used to simulate visibility reduction associated with a major dust-storm that caused a 164-vehicle accident on Interstate 5 in California. Finally, long-term dust hours predictions were made for Lubbock, Texas. Predictions compared favorably with measured data. It is concluded that the Texas Tech Erosion Analysis Model (TEAM) is a reasonable tool for the simulation and analysis of wind erosion and dust generation.

References

Abtew, W., J.M. Gregory, and J. Borrelli. 1989. Wind profile: Estimation of Displacement Height and Aerodynamic Roughness. *Transactions of the ASAE*. 32(2):521-527.

Anderson, R.S. and B. Hallet. 1986. Sediment Transport by Wind: Toward a General Model. *Geological Society of America Bulletin.* 97:523-535.

Bagnold, R.A. 1936. The Movement of Desert Sand. *Proceedings of the Royal Society of London,* A 157, pp. 594-620.

Bagnold, R.A. 1941. *The Physics of Blown Sand and Desert Dunes.* Methuen, London.

Bisel, F. and J. Hsieh. 1966. Influence of Soil Moisture on the Erodibility of Soil by Wind. *J. of Soil Sci.* 102:143-146.

Chepil, W.S. 1956. Influence of Moisture on Erodibility of Soil by Wind. *Proceedings of the Soil Sci. Soc. Am.* 20:288-292.

Chepil, W.S. 1957. Width of Field Strip to Control Wind Erosion. Kansas Agricultural Experiment Station Technical Bulletin 92. Kansas State University. Manhattan, Kansas.

Chepil, W.S. and N.P. Woodruff. 1963. The Physics of Wind Erosion and its Control. *Advances in Agronomy*. 15:211-302.

Darwish, M.M. 1991. The effects of Soil Moisture and Particle Size on Threshold Friction Velocity. M.S. Thesis. Texas Tech University, Lubbock, Texas.

Greeley, R. and J.D. Iversen. 1985. *Wind as a geological process on Earth, Mars, Venus and Titan.* Cambridge University Press, Cambridge.

Gregory, J.M. 1982. Soil Cover Prediction with Various Amounts and Types of Crop Residue. *Transactions of the ASAE.* 25(5):1333-1337.

Gregory, J.M. 1984a. Prediction of Soil Erosion by Water and Wind for Various Fractions of Cover. *Transactions of the ASAE*. 27(5):1345-1350, 1354.

Gregory, J.M. 1984b. Analysis of the Length Effect for Soil Erosion by Wind. Paper presented at the Winter meeting of ASAE, New Orleans, LA. Paper No. 842540.

Gregory, J.M. 1987. Visibility Prediction from Dust Concentration and Particle Size. Presented at the Summer Meeting of the ASAE, Baltimore, MD. Paper No. 872032.

Gregory, J.M. 1991. Wind Erosion: Prediction and Control. Report prepared for the US Army Corps of Engineers, Waterways Experiment Station, Vicksburg, MS.

Gregory, J.M. 1992. Erosion Equation Derivation Similar to the USLE. Paper presented at the Summer Meeting of the ASAE, Charlotte, NC. Paper No. 922051.

Gregory, J.M. and M.M. Darwish. 1990. Threshold Friction Velocity Prediction Considering Water Content. Paper presented at the Winter Meeting of the ASAE, Chicago, IL. Paper No. 902562.

Gregory, J.M., U.B. Singh, J.A. Lee, and C.B. Fedler. 1991. Dust Hours, Visibility, and Wind Erosion Prediction. Paper presented at the Summer Meeting of the ASAE, Albuquerque, NM. Paper No. 914007.

Gregory, J.M., G.R. Wilson, and U.B. Singh. 1993a. Wind Erosion: Detachment and Maximum Transport Rate. Paper presented at the Summer Meeting of the ASAE, Spokane, WA. Paper No. 932050.

Gregory, J.M., U.B. Singh, and G.R. Wilson. 1993b. PM_{10} Prediction: Problems and Strategies. Paper presented at the Winter Meeting of the ASAE, Chicago, IL. Paper No. 932541.

Gregory, J.M., J.A. Lee, G.R. Wilson, and U.B. Singh. 1993. Modeling Seasonal Patterns of Blowing Dust on the Southern High Plains. 3rd International Geomorphology Conference, Hamilton, Ontario, Canada.

Gregory, J.M., G.R. Wilson, and U.B. Singh. 1996. The Physics of Wind Erosion and Dust Generation. Paper presented at the Fifth International Conference on Desert Development: The Endless Frontier. August 12-17. Texas Tech University, Lubbock, Texas.

Layton, J.B., E.L. Skidmore, and C.A. Thompson. 1993. Winter-Associated Changes in Dry-Soil Aggregation and Influenced by Management. *Soil Science Society of America Journal*. 57:1568-1572.

Nickling, W.G. 1978. Eolian Sediment Transport During Dust Storms: Slims River Valley, Yukon Territory. *Canadian Journal of Earth Science*. 15:1069-84.

Owen, P.R. 1964. Saltation of Uniform Grains in Air. *Journal of Fluid Mechanics*. 20:225-242.

Pehrson, J.R. and J.D. Chiou. 1996. Emissions of Contaminated Fugitive Dust Under Extreme (Non-Tornado) Wind Conditions. Proceedings of the Topical Meetings on The Best of R &D. American Nuclear Society, Inc. La Grange Park, Illinois 60526.

Puri, A.N., E.. Crowther, and B.A. Keen. 1925. The Relation Between the Vapor Pressure and Water Content of Soils. *J Ag. Sci*. 15:68-88.

Robinson, E. 1968. Effects of Air Pollution on Visibility. *In Air Pollution*. Edited by A.C. Stern. Vol. 1, Chapter 2. Academic Press, New York.

Singh, U. B., J.M. Gregory, G.R. Wilson, R.E. Peterson, and C.B. Fedler. 1992. Climate Change Effects on Wind Erosion. Paper presented at the Summer Meeting of the ASAE. Paper No. 922050.

Singh, U.B. 1994. Wind Erosion: Mechanics of Saltation and Dust Generation. Ph.D. Thesis. Department of Civil Engineering, Texas Tech University, Lubbock, Texas.

Skidmore, E.L. and D.H. Powers. 1982. Dry Soil-Aggregate Stability: Energy-Based Index. *Soil Science Society of America Journal.* 46(6):1274-1279.

Skidmore, E.L. and J.B. Layton. 1992. Dry-Soil Aggregate Stability as Influenced by Selected Soil Properties. *Soil Science Society of America Journal*. 56:557-561.

Svasek, J.N. and J.H.J. Terwindt. 1974. Measurements of Sand Transport by Wind on a Natural Beach. *Sedimentology*. 21:311-22.

Wilson, G.R. 1994. Modeling Wind Erosion: Detachment and Maximum Transport Rate. Unpublished Ph.D. Dissertation, Texas Tech University, Lubbock, TX 79409.

Wilson, G. R. and J. M. Gregory. 1992. Soil Erodibility: Understanding and Prediction. Paper presented at the Summer Meeting of the ASAE. Charlotte, NC. Paper No. 922049.

Wilson, G.R., J.R. Brownell, and J.M. Gregory. 1993a. Analysis of Dust Triggered Accident on Interstate 5. Presented at the Summer Meeting of the ASAE, Spokane, WA. Paper No. 932117.

Wilson, G.R., T.M. Zobeck, J.M. Gregory, and R.E. Zartman. 1993b. Sediment Transport by Wind: A Wind Tunnel Study. Paper presented at the Winter Meeting of the ASAE, Chicago, IL. Paper No. 932542